JOURNAL OF GUIDANCE, CONTROL, AND DYNAMICS
Vol. 32, No. 4, July–August 2009

Spacecraft Trajectory Optimization Based on Discrete Sets of Pseudoimpulses

Yuri Ulybyshev*
Rocket-Space Corporation "Energia," Korolev, Moscow Region, 141070, Russia

DOI: 10.2514/1.41201

A brief review of new methods for continuous-thrust trajectory optimization is presented. The methods use discretization of the spacecraft trajectory on segments and sets of pseudoimpulses for each segment. Boundary conditions are presented as a linear matrix equation. A matrix inequality on the sum of the characteristic velocities for the pseudoimpulses is used to transform the problem into a large-scale linear programming form. Present-day linear programming methods use interior-point algorithms to solve such problems. In the general case, the continuous burns include a number of adjacent segments and a postprocessing of the linear programming solutions is needed to form a sequence of the burns. An optimal number of the burns is automatically determined in the postprocessing. The methods provide flexible opportunities for the trajectory computation in complex missions with various requirements and constraints. A systematic mathematical representation of these problems is considered. A summary of examples for orbit transfer, rendezvous, and moon ascent trajectories is presented. Application examples of lunar landing trajectories are examined. The examples represent a set of optimal unconstrained trajectories for different thrust-to-weight ratios and trajectories with safety descent profile, thrust level, and attitude constraints.

Nomenclature

$\mathbf{A}$	=	matrix of inequality constraints
$\mathbf{A_e}$	=	matrix of partial derivatives
a	=	thrust acceleration
a_o	=	initial thrust acceleration
$\mathbf{b}$	=	vector of inequality constraints
$\mathbf{e}$	=	thrust-direction unit vector
$\mathbf{F}$	=	boundary-condition function
f_T	=	dimensionless thrust level
$\mathbf{g}$	=	vector of gravitational acceleration
g_M	=	gravitational acceleration on the moon surface
h	=	altitude
I_{sp}	=	specific impulse
i	=	segment number
J	=	performance index
j	=	pseudoimpulse number
k	=	quantity of pseudoimpulses at each segment
L	=	horizontal range
M	=	spacecraft dimensionless mass (for initial time $M \equiv 1$)
$\dot{M}$	=	dimensionless mass rate for maximum thrust level
m	=	number of boundary conditions
n	=	quantity of segments
$\mathbf{P_f}$	=	vector of boundary conditions
$\mathbf{P_f^*}$	=	vector of boundary parameters along the trajectory without any maneuvers
$\mathbf{r}$	=	radius vector
Q	=	function of interior-point inequality constraints
$\mathbf{q}$	=	weight coefficient vector of the fuel usage for the segments
t	=	time
$\mathbf{V}$	=	spacecraft velocity vector
$\mathbf{X}$	=	vector of decision variables
$\mathbf{Y}$	=	state vector
$\Delta\mathbf{P_f}$	=	target vector
Δt_i	=	duration of the ith segment
$\Delta\mathbf{V}_{\mathbf{i}\mathrm{opt}}$	=	optimal characteristic velocity vector at the ith segment
$\Delta V_i^{(j)}$	=	dimensionless characteristic velocity of the jth pseudoimpulse at the ith segment
ΔV_X	=	characteristic velocity
ϑ	=	thrust angle
φ	=	pitch angle

Presented as Paper 6276 at the AIAA/AAS Astrodynamics Specialist Conference, Honolulu, HI, 18–21 August 2008; received 25 September 2008; revision received 28 February 2009; accepted for publication 2 March 2009.

*Head of Space Ballistic Department; yuri.ulybyshev@rsce.ru. Senior Member AIAA.

I. Introduction

THE optimization problem of continuous-thrust spacecraft trajectories has been studied extensively [1–18]. The optimization methods for the trajectories have been mainly of two types: indirect and direct techniques or their combinations. Indirect methods attempt to solve a two-point boundary-value problem based on the Pontryagin maximum principle [19]. In the boundary-value problem, the unknown costate variables are very sensitive and difficult to guess. Direct methods convert the problem into parameter optimization, which is in turn solved using, as a rule, nonlinear programming methods [2]. The methods are attractive because explicit consideration of the necessary optimal conditions (adjoint equations and transversality conditions) is not required. A general review of space trajectory optimization methods was presented by Betts [20].

Linear programming represents one of the well-known optimization methods successfully used to solve many complex application problems in engineering, economics, and operations research. But classical linear programming has not been practically used for the optimization of continuous-thrust trajectories. Ulybyshev and Sokolov [9] have developed a method for optimization of many-revolution, low-thrust maneuvers in the vicinity of the geostationary orbit. The method uses pseudomaneuvers with either positive or negative transverse directions for every trajectory segment (half a revolution) so that it is possible to state the problem in terms of classical linear programming with a number of decision variables equal to quadruple the number of revolutions in the orbit transfer.

In the 1990s, linear programming underwent a revolution with the development of polynomial-time algorithms known as interior-point methods [21–23] that perform more effectively than the classical simplex methods. Furthermore, unlike simplex-based algorithms that have difficulty with degenerate problems, interior-point methods are immune to degeneracy [22]. This makes it possible to develop effective methods that use large-scale linear programming for spacecraft trajectory optimization.

The new methods are based on two ideas. The first is a well-known discretization of time, in the general case, on nonuniform segments. The second is the key idea, based on a near-uniform discrete approximation of a control space (i.e., thrust direction and magnitude) by a set of pseudoimpulses with an inequality constraint for each segment.

In a sense, the paper is a continuation of the author's previous works [16–18] in which the key idea was used for optimization of continuous-thrust trajectories. The paper contains three major parts. First is a general presentation of the methods. A systematic mathematical representation of a trajectory optimization problem for the most commonly used requirements and constraints is also considered. Second is a brief review of major qualitative and computational features for several application examples: maintenance of a 24 h elliptical orbit, coplanar and noncoplanar orbit transfers, various rendezvous trajectories for near-circular orbits (with high, medium, and low thrust), and a three-dimensional launch trajectory from the moon's surface to a circumlunar orbit with constraints. New application examples of lunar landing trajectories are considered in the last part: a set of optimal unconstrained trajectories for different thrust-to-weight ratios and trajectories with safety descent profile, thrust level, and attitude constraints.

II. Spacecraft Trajectory Optimization in Linear Programming Form

A. Spacecraft Motion Model

We consider a point-mass spacecraft with a limited thrust. The equations of the spacecraft motion can be expressed as

$$\frac{d\mathbf{Y}}{dt} = \mathbf{f}[\mathbf{Y}(t), f_T(t), \mathbf{e}(t), M] \tag{1}$$

where

$$\mathbf{Y}^{\mathbf{T}}(t) = [\mathbf{r}^{\mathbf{T}}(t), \mathbf{V}^{\mathbf{T}}(t), M(t)] \tag{2}$$

$$\mathbf{f}\,[\mathbf{Y}(t), f_T(t), \mathbf{e}(t), M(t)] = \begin{Bmatrix} \mathbf{V}(t) \\ \mathbf{g} + f_T \frac{a_0}{M}\mathbf{e}(t) \\ -f_T \dot{M} \end{Bmatrix} \tag{3}$$

The controls are defined as the thrust direction $\mathbf{e}$ and thrust level f_T. The optimal control problem formulation considered here is to minimize a performance index that is the total characteristic velocity.

Terminal conditions for the trajectory are

$$\mathbf{F}\,[\mathbf{Y}(t_{f1}), \mathbf{Y}(t_{f2}), \ldots, \mathbf{Y}(t_f)] = \mathbf{P}_f \tag{4}$$

where $\mathbf{F}$ is a vector function of a state vector at the final time and, in the general case, at interior points of the trajectory t_{f1}, t_{f2}, etc.; $\mathbf{P}_f$ is an m dimension specified vector of the boundary conditions.

B. Trajectory Discretization

Introduce a set of segments as the partition $[t_0, t_1, t_2, \ldots, t_n]$, with $t_0 = 0$ and $t_n = t_f$. The mesh points t_i are referred to as nodes, the intervals $\Delta t_i = [t_{i+1}, t_i]$ are referred to as trajectory segments. In the general case, the segments can be nonuniform. Suppose that approximate values of the state vectors at the nodes $\mathbf{Y}(t_i)$ are known, then for the constant controls at each segment, we can write

$$\begin{aligned} \mathbf{P_f}(t_f) &= \mathbf{P}^*_{\mathbf{f}}(t_f) + \sum_{i=1}^{n} \frac{\partial \mathbf{F}(t_i)}{\partial \mathbf{V}} \cdot \frac{f_{Ti} a_0 \mathbf{e}_i \Delta t_i}{M_i} \\ &= \mathbf{P}^*_{\mathbf{f}}(t_f) + \sum_{i=1}^{n} \frac{\partial \mathbf{F}(t_i)}{\partial \mathbf{V}} \cdot \Delta V_{xi} \mathbf{e}_i \end{aligned} \tag{5}$$

where $\mathbf{P}^*_f$ is a vector of the boundary parameters computed along a trajectory without any maneuvers, $\partial \mathbf{F}(t_i)/\partial \mathbf{V}$ is a matrix of partial derivatives, and $0 \le \Delta V_{xi} \le \Delta V_{xi\,\max}$ is the characteristic velocity for the ith segment. In a sense, Eq. (5) represents a simple form of the well-known Encke's method [24], which uses integration of only the difference from a known reference trajectory.

Note that the final time t_f and segment durations Δt_i may be defined in an implicit form.

C. Sets of Pseudoimpulses

The simplest case of the control space for the thrust vector is a plane. As an example, it can be a local horizontal or orbit plane. We consider an ith segment independent of all the other segments. Suppose that the thrust direction in the plane is arbitrary. Without loss of generality, let a dimensionless characteristics velocity or impulse for the segment be $\Delta V_{xi} \le 1$. All of the possible thrust directions can be present as a set of pseudoimpulses $\mathbf{e}_i^{(j)}$ within the unit circle with a small angle of $\Delta\varphi = 2\pi/k$ between them (Fig. 1a). Suppose that there is an optimal impulse $\Delta \mathbf{V}_{i\mathrm{opt}}$ for the ith segment.

Thus, we can present the optimal impulse by the sum

$$\Delta \mathbf{V}_{i\mathrm{opt}} = \sum_{1}^{k} \Delta V_i^{(j)} \mathbf{e}_i^{(j)} \tag{6}$$

with a constraint for the characteristic velocities of the pseudoimpulses (Fig. 1b):

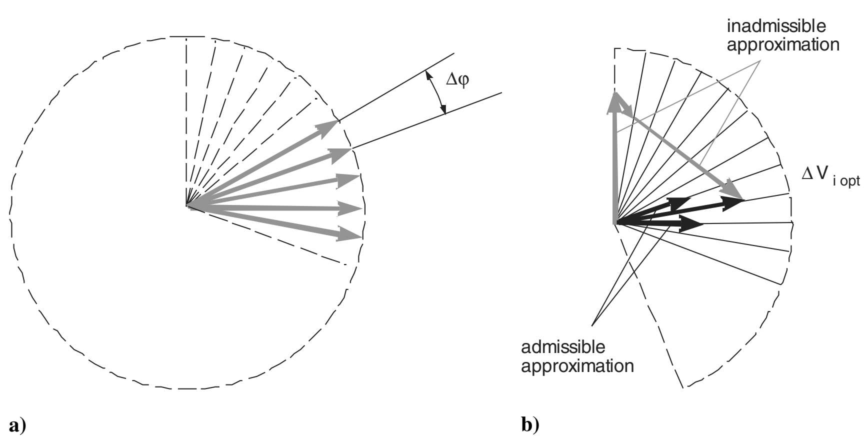

Fig. 1 Set of pseudoimpulses in a plane.

$$\sum_{1}^{k} \Delta V_i^{(j)} \leq 1 \tag{7}$$

It is evident that the optimal vector approximation of the optimal impulse by the pseudoimpulses is a sum of the two nearest-neighbor pseudoimpulses.

In a similar way, we consider a three-dimensional case for the possible thrust directions. A set of pseudoimpulses can be constructed using a uniform distribution on the unit sphere. Examples of such sets on the full sphere and on a spherical segment are depicted in Fig. 2. Similarly to the planar case, for each segment, the sum of characteristic velocities of the pseudoimpulses should be constrained by the inequality (7). The best approximation of an optimal impulse $\Delta \mathbf{V}_{i\mathrm{opt}}$ is also a sum of nearest-neighbor pseudoimpulses.

D. Transformation to Basic Linear Programming Form

Define a $(n \times k)$-dimension vector of decision variables:

$$\mathbf{X}^{\mathrm{T}} = [\Delta V_1^{(1)}, \Delta V_1^{(2)}, \ldots, \Delta V_1^{(k)}, \Delta V_2^{(1)}, \Delta V_2^{(2)}, \ldots, \Delta V_2^{(k)}, \ldots, \Delta V_n^{(k)}] \tag{8}$$

It should be noted that all the vector components must be nonnegative. For the vector, according to the previous statements, the following linear inequality can be written

$$\mathbf{AX} \leq \mathbf{b} \tag{9}$$

where $\mathbf{A}$ is a $n \times (n \times k)$-dimension matrix of the following form (all of the unspecified elements equal to zero),

$$\mathbf{A} = \underbrace{\begin{bmatrix} \underbrace{111\cdots1}_{k} & & & \\ & \underbrace{111\cdots1}_{k} & & \\ & & \ddots & \\ & & & \underbrace{111\cdots1}_{k} \end{bmatrix}}_{n\times k} \Bigg\} n \tag{10a}$$

and an n-dimension vector:

$$\mathbf{b}^{\mathrm{T}} = [1, 1, 1, \ldots, 1, 1] \tag{10b}$$

For the decision-variable vector $\mathbf{X}$, the boundary conditions from Eq. (5) can be expressed as

$$\Delta \mathbf{P}_f = \mathbf{P}_f - \mathbf{P}_f^* = \mathbf{A_e X} \tag{11}$$

where $\Delta \mathbf{P}_f$ is a target vector, and $\mathbf{A_e}$ is a $m \times (n \times k)$-dimension matrix of partial derivatives:

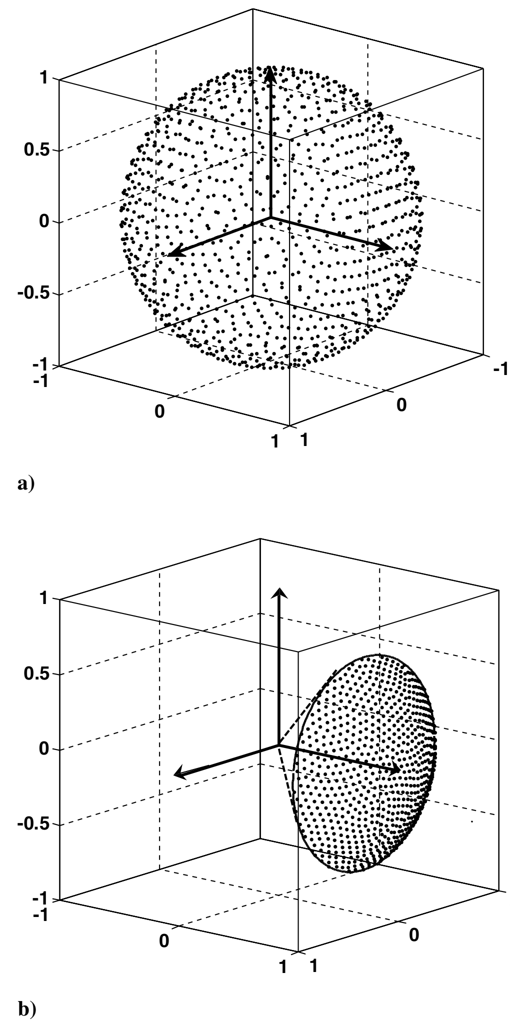

Fig. 2 Near-uniform point distributions in 3-D space.

$\Delta t_{2\max}, \ldots, \Delta t_{n\max}]$ for the unequal segments. Then a performance index corresponding to the minimum characteristic velocity of the transfer can be written as

$$J = \min(\mathbf{q}^{\mathbf{T}} \cdot \mathbf{X}) \tag{13}$$

As a result, we have a classical linear programming problem with constraints of a linear inequality and equality given by Eqs. (9) and (11), respectively. The elements of the decision-variable vector $\mathbf{X}$ must be nonnegative and constrained:

$$0 \leq \Delta V_i^{(j)} \leq 1 \tag{14}$$

$$\mathbf{A}_{\mathbf{e}} = \begin{bmatrix} \underbrace{\frac{\partial F_1}{\partial V_1^{(1)}} \; \frac{\partial F_1}{\partial V_1^{(2)}} \cdots \frac{\partial F_1}{\partial V_1^{(k)}}}_{k} & \underbrace{\frac{\partial F_1}{\partial V_2^{(1)}} \; \frac{\partial F_1}{\partial V_2^{(2)}} \cdots \frac{\partial F_1}{\partial V_1^{(k)}}}_{k} & \cdots & \underbrace{\frac{\partial F_1}{\partial V_n^{(1)}} \; \frac{\partial F_1}{\partial V_n^{(2)}} \cdots \frac{\partial F_1}{\partial V_n^{(k)}}}_{k} \\ \underbrace{\frac{\partial F_2}{\partial V_1^{(1)}} \; \frac{\partial F_1}{\partial V_1^{(2)}} \cdots \frac{\partial F_2}{\partial V_1^{(k)}}}_{k} & \underbrace{\frac{\partial F_2}{\partial V_2^{(1)}} \; \frac{\partial F_2}{\partial V_2^{(2)}} \cdots \frac{\partial F_2}{\partial V_2^{(k)}}}_{k} & \cdots & \underbrace{\frac{\partial F_2}{\partial V_n^{(1)}} \; \frac{\partial F_2}{\partial V_n^{(2)}} \cdots \frac{\partial F_2}{\partial V_n^{(k)}}}_{k} \\ \vdots & \vdots & \vdots & \vdots \\ \underbrace{\frac{\partial F_m}{\partial V_1^{(1)}} \; \frac{\partial F_m}{\partial V_1^{(2)}} \cdots \frac{\partial F_m}{\partial V_1^{(k)}}}_{k} & \underbrace{\frac{\partial F_m}{\partial V_2^{(1)}} \; \frac{\partial F_m}{\partial V_2^{(2)}} \cdots \frac{\partial F_m}{\partial V_2^{(k)}}}_{k} & \cdots & \underbrace{\frac{\partial F_m}{\partial V_n^{(1)}} \; \frac{\partial F_m}{\partial V_n^{(2)}} \cdots \frac{\partial F_m}{\partial V_1^{(k)}}}_{k} \end{bmatrix} \tag{12}$$

where $\partial F_q / \partial V_i^{(j)}$ is a partial derivative that can be computed using analytical relations or numerically.

Introduce a $(n \times k)$-dimension vector of weight coefficients as $\mathbf{q}^{\mathbf{T}} = [1 \quad 1, \ldots, 1 \quad 1]$ for the equal segments or as $\mathbf{q}^{\mathbf{T}} = [\Delta t_{1\max},$

The presented linear programming form is a large-scale problem but modern scientific software, such as MATLAB®, contains effective algorithms for sparse matrix computations [25] including large-scale linear programming.

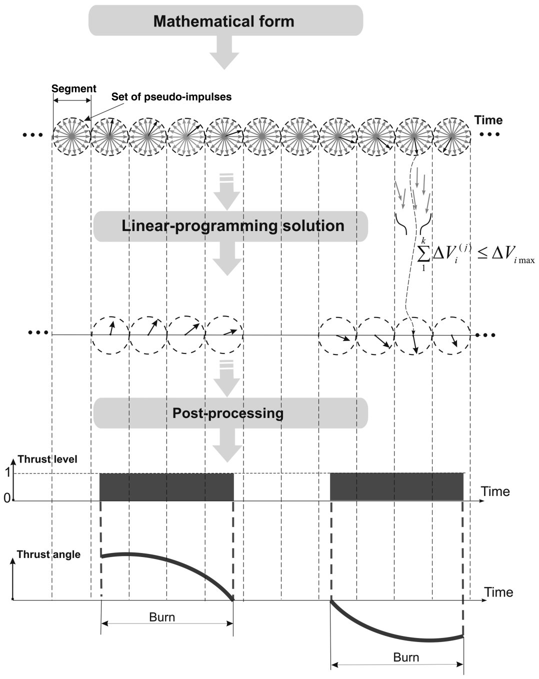

Fig. 3 Postprocessing of the linear programming solutions.

E. Postprocessing of Linear Programming Solutions

It is evident that the segments in the linear programming form are formally considered independent of each other. Therefore, an additional postprocessing and validation are required for the linear programming solutions (see Fig. 3). It is necessary to find all of the segments corresponding to the nonzero decision variables. The adjacent segments among these should be joined in burns. If two (or three in the three-dimensional case) decision variables belong to a segment, then the thrust magnitude and direction should be computed from the vector sum of the corresponding pseudo-impulses. It should be noted that the optimal number of burns is automatically determined in the postprocessing. Other qualitative aspects of solutions and their relation with the primer vector theory [26] are described in [16–18].

F. Iterative Solutions and Nonlinear Problems

In a sense, the spacecraft trajectories can be divided into two categories: a motion near a reference trajectory and a general case with substantial change of initial trajectory parameters and, respectively, the partial derivatives. For the first, the partial derivatives in Eq. (12) are known with a relatively high precision. For the second, an intermediate trajectory and, respectively, the partial derivatives in Eq. (12), are usually not known a priori. For this case, we can use an iterative technique with a refinement of the partial derivatives at each iteration. For the first iteration we define an initial guess for intermediate trajectory parameters. As an example, it can be a linear time variation between initial and target parameters. Based on the linear programming solution, the parameters are refined for the second iteration, etc., to satisfy the specified boundary conditions. Usually, iterative solutions are also needed for linear problems with spacecraft mass variation. It is significant that the iterative processes for the proposed method contain attractive features. Unknown intermediate trajectory parameters have, as a rule, monotonic variations and/or known variation ranges between the initial and target parameters. Contrary to the methods presented here, the optimal control techniques in the form of an iterative solution for a two-point boundary-value problem for the state and adjoint variables are difficult to apply. The main difficulty with these methods is getting started (i.e., finding a first estimation of the unspecified conditions for the state and adjoint variables [27]). Moreover, the adjoint variables do not have a physical meaning, and thus, it can be difficult to find a reasonable initial guess for them [27]. An application of the presented method to nonlinear problems would require additional study, but [16] presents some examples of a related method to nonlinear problems in continuous-thrust systems. We believe that a feasible way to solve nonlinear problems is computation of the partial derivatives in Eq. (12) based on techniques for approximate determination of trajectory arcs [28].

The interior-point methods are not only highly efficient algorithms for the large-scale linear programming, but they are immune to degeneracy [22]. Therefore, the absence of a solution with a low thrust means, most likely, that the thrust acceleration (i.e., the spacecraft thrust-to-weight ratio) is small for the trajectory, or the problem formulation with the boundary conditions and constraints is degenerate. For the last case, an attempt of the solution for a very-high-thrust acceleration can be used as a validation test of the possible degeneracy. Such validation is very important for spacecraft design analysis.

G. Optimization of Constrained Trajectories

The basic form of the trajectory optimization problem without constraints was presented in the previous section. The real space missions are often required to satisfy not only terminal conditions, but also some specific requirements. As examples, there are constraints for interior points in the form of boundary conditions or inequalities; constraints or preferences for some thrust directions; burn intervals; use of a multimode propulsion system with a combination of high, medium, and/or low thrust; and other operational constraints. It is significant that the methods provide flexible opportunities for computation and design of optimal trajectories with various requirements and constraints. For such complex missions, an extension and/or modification of the basic linear programming form is required (i.e., transformation of the matrices $\mathbf{A}$, $\mathbf{A_e}$, the weight vector $\mathbf{q}$, set of segments, and/or sets of pseudoimpulses). A schematic diagram in Fig. 4 illustrates the transformations for most used requirements and constraints.

Each l dimension interior-point equality constraint of $\mathbf{F}_{\mathrm{IP}}[Y(t_{f\mathrm{IP}})] = \mathbf{P}_{\mathrm{IP}}$ needs additional rows in the matrix $\mathbf{A_e}$:

$$\mathbf{A_e} = \left[\overbrace{\frac{\partial \mathbf{F}_{\mathrm{IP}}}{\partial V_1^{(1)}} \quad \frac{\partial \mathbf{F}_{\mathrm{IP}}}{\partial V_1^{(2)}} \quad \cdots \quad \frac{\partial \mathbf{F}_{\mathrm{IP}}}{\partial V_\tau^{(k-1)}} \quad \frac{\partial \mathbf{F}_{\mathrm{IP}}}{\partial V_\tau^{(k)}}}^{\mathbf{A}'_{\mathbf{e}}} \quad \mathbf{O}_{l\times[(n-1)\times k]} \right] \tag{15}$$

where $\mathbf{A}'_{\mathbf{e}}$ is the matrix in Eq. (12), $\mathbf{O}_{l\times[(n-1)\times k]}$ is the zero matrix, and τ is an index of the last segment preceding the instant $t_{f\mathrm{IP}}$. In this case, the matrix $\mathbf{A_e}$ has dimension of $(l+m)\times(n\times k)$.

An inequality constraint related to an engine time $\Delta t_{E\max}$ at a time subinterval (as an example for spacecraft using electrojet engines) is presented as a quantity of the adjacent segments corresponding to the subinterval with an extension of the matrix $\mathbf{A}$ and vector $\mathbf{b}$ as

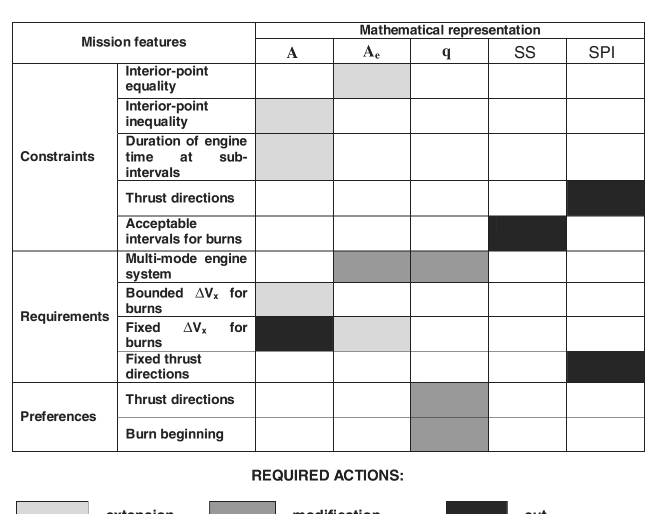

Fig. 4 Constraint representations (SS: set of segments and SPI: set of pseudoimpulses).

$$\mathbf{A} = \begin{bmatrix} & & & \mathbf{A}' & & & \\ \mathbf{O}_{1\times[(l-1)\times k]} & \underbrace{\Delta t_{l\max} \quad \cdots \quad \Delta t_{l\max}}_{k} & & \cdots & \underbrace{\Delta t_{s\max} \quad \cdots \quad \Delta t_{s\max}}_{k} & \mathbf{O}_{1\times[(n-s)\times k]} \end{bmatrix} \tag{16a}$$

$$\mathbf{b}^{\mathbf{T}} = [1, 1, 1, \ldots, 1, 1, \Delta t_{E\max}] \tag{16b}$$

where $\mathbf{A}'$ is the base matrix as in Eq. (10a), and $\mathbf{O}_{1\times[(l-1)\times k]}$ and $\mathbf{O}_{1\times[(n-s)\times k]}$ are zero string vectors.

More general interior-point inequality constraints are

$$Q[\mathbf{Y}(t)] \leq 0 \quad \text{for } 0 \leq t_b \leq t \leq t_e \leq t_f \tag{17}$$

where t_b and t_e are the start and end times of a constrained trajectory part. The problem must be treated as a sequence of constrained segments. Suppose that s is the first segment for that $t_b \leq t_s$ and $s + m$ is the last segment for that $t_{s+m} \leq t_{e,}$. In addition to Eq. (9), we have the following m inequalities:

$$Q(t_l) = Q^*(t_l) + \sum_{i=1}^{i=l} \sum_{j=1}^{k} \frac{\partial Q}{\partial V_i^{(j)}} \cdot \Delta V_i^{(j)} \leq 0 \tag{18}$$

where $s \leq l \leq s + m$ is the segment index for the interval between t_b and t_e, $Q^*(t_l)$ is the function (17) computed along free trajectory, and $\partial Q/\partial V_i^{(j)}$ is a partial derivative. Therefore, the matrix $\mathbf{A}$ (10a) with a dimension of $(n + m) \times (n + k)$ can be expressed as (all of the unspecified elements equal to zero)

A complex example with interior-point inequality constraints for a time interval, thrust level, and attitude constraints is given subsequently.

III. Summary of Examples for Orbit Transfer, Rendezvous, Moon Ascent Trajectories

Major qualitative and computational features of various application examples from [16–18] are presented in the Table 1. The first example is the maintenance of a 24 h elliptical orbit. It is an optimization of station-keeping maneuvers in a neighborhood of the orbit for a spacecraft with possible thrust directions in the local horizontal plane. The second and third examples are coplanar and noncoplanar orbit transfers with thrust directions in the orbit plane and three-dimensional space, respectively. The next example is optimization of rendezvous trajectory near circular orbits for spacecraft with low-thrust propulsion system. The example includes equality interior-point constraints related to execution of a flyby around the passive spacecraft before rendezvous accomplishment. Three-dimensional launch trajectories from the moon surface to a circumlunar orbit with constraints are considered in the last example.

IV. Trajectory Optimization for Lunar Landing

A. Lunar Lander Motion Equations

Motion of a lunar landing spacecraft can be modeled by a variable-mass point moving over a flat surface with a uniform gravity field:

$$\mathbf{A} = \begin{bmatrix} 111,\ldots,1 & & & & & & & & \\ & 111,\ldots,1 & & & & & & & \\ & & \ddots & & & & & & \\ & & & 111,\ldots,1 & & & & & \\ & & & & 111,\ldots,1 & & & & \\ & & & & & \ddots & & & \\ & & & & & & 111,\ldots,1 & & \\ & & & & & & & 111,\ldots,1 & \\ & & & & & & & & \ddots \\ & & & & & & & & & 111,\ldots,1 \\ \mathbf{A}_{n+1,1} & \mathbf{A}_{n+1,2} & \cdots & \mathbf{A}_{n+1,s} & & & & & \\ \mathbf{A}_{n+2,1} & \mathbf{A}_{n+2,2} & \cdots & \mathbf{A}_{n+2,s} & \mathbf{A}_{n+2,s+1} & & & & \\ \vdots & \vdots & \vdots & \vdots & \vdots & \ddots & & & \\ \mathbf{A}_{n+m,1} & \mathbf{A}_{n+m,2} & \cdots & \mathbf{A}_{n+m,s} & \mathbf{A}_{n+m,s+1} & \cdots & \mathbf{A}_{n+m,s+m} & & \end{bmatrix} \tag{19}$$

where

$$\mathbf{A}_{n+l,i} = \begin{bmatrix} \partial Q/V_i^{(1)} & \partial Q/V_i^{(2)} & \cdots & \partial Q/V_i^{(k)} \end{bmatrix} \tag{20}$$

is a k-dimension row vector of partial derivatives. The $(n + m)$-dimension vector $\mathbf{b}$ in Eq. (10b) is

$$\mathbf{b}^{\mathbf{T}} = \begin{bmatrix} 1 & 1 & 1 & \cdots & 1 & -Q^*(t_s) & -Q^*(t_{s+1}) & \cdots & -Q^*(t_l) & \cdots & -Q^*(t_{s+m}) \end{bmatrix} \tag{21}$$

Thrust-direction constraints can be considered in an explicit form through corresponding sets of pseudoimpulses. Preferences for thrust directions and/or modes of the propulsion system are presented in an explicit form through the weight vector $\mathbf{q}$. Some examples of mission features are given in [16–18]. It is significant that the aforementioned requirements and constraints can be considered not only separately, but also in combination with each other.

$$\begin{cases} \frac{dh}{dt} = V_h \\ \frac{dL}{dt} = V_L \\ \frac{dV_h}{dt} = f_T \frac{a_0}{M} \sin\varphi - g_M \\ \frac{dV_L}{dt} = f_T \frac{a_0}{M} \cos\varphi \\ \frac{dM}{dt} = -f_T \dot{M} \end{cases} \tag{22}$$

Table 1 Application examples summary[a]

Trajectory	Duration	Solution type	Partial derivatives model	Mass model	Constraints	Segment	Thrust directions, k	n	Number of: Decision variables	Number of: Nonzero variables	Number of: Burns
HEO station- keeping	30 days	Linear	Near elliptical orbit	Constant	D	Arc of 10 deg in true anomaly	In-plane, 36	1080	38,880	~900	~60
LT transfer from GTO to GEO	29 days	Nonlinear, iterative	Inverse-square gravity field	Constant	—	One burn	In-plane, 360	80	28,280	46	46
MT noncoplanar transfer	8.6 h	Nonlinear, iterative	Inverse-square gravity field	Constant	—	Arc of 10 deg in argument of latitude	3-D, 1000	72	72,000	1713	3
LT rendezvous with flyby	30 revolutions	Linear	Near-circular orbit	Constant	IP	150 s	In-plane, 61	1080	65,880	515	60
Noncoplanar launch to moon orbit	560 s	Linear, iterative	Uniform gravity	Variable	TD, D	4 s	3-D in hemisphere 2799	140	391,860	~140	2

[a]The abbreviations in the table are as follows: HEO: high elliptical orbit; GEO: geostationary orbit; GTO: geotransfer orbit; LT and MT: low and medium thrust, respectively; D: constraints on engine time at time subintervals; IP: interior-point equality constraints; TD: thrust-direction constraints; and 3-D: three-dimensional space.

The control variables are $f_T(t)$ and $\varphi(t)$. Soft-landing terminal conditions for a specified terminal time t_f are

$$\mathbf{P}^{\mathbf{T}}(t_f) = [h_f, V_{hf}, V_{Lf}]^{\mathbf{T}} = [0, 0, 0]^{\mathbf{T}} \tag{23}$$

Let us suppose that the sets of segments and pseudoimpulses are defined and that approximate mass values M_i at the segments are known. Then for the partial derivatives in the matrix $\mathbf{A_e}$ (12), we can write

$$\frac{\partial \mathbf{F}}{\partial V_i^{(j)}} = \frac{a_0 f_{Ti} \Delta t_i}{M_i} \begin{bmatrix} (t_f - t_i)\sin\varphi^{(j)} \\ \sin\varphi^{(j)} \\ \cos\varphi^{(j)} \end{bmatrix} \tag{24}$$

An iterative process is required for refinement of the mass M_i at the segments and, respectively, the partial derivatives. As a rule, to obtain the converged values, only two or three iterations are needed in this computation. For the next application examples, a spacecraft in a circular orbit of 100 km altitude and with an engine specific impulse of $I_{\mathrm{sp}} = 350$ s is considered.

B. Set of Optimal Unconstrained Trajectories

As a lower bound of the required characteristic velocity for lunar landing trajectories, a set of optimal unconstrained trajectories for different initial thrust accelerations (or thrust-to-weight ratios) can be used. Figure 5 shows the required ΔV_x versus the specified landing time.

The results are given for different values of a_0 (in m/s^2), $\Delta t_i = 2.5$ s, and 360 uniformly distributed pseudoimpulses on the unit circle are used for all segments. For each a_0, there are the two extreme solutions in terms of the required characteristic velocity and landing time. The first is the minimum-time solution $t_{f\,\min}$. In this case, we have a trajectory with a continuous maximum thrust. The second is a trajectory with the minimum required ΔV_x and a landing time $t_{fV} > t_{f\,\min}$. The difference between these solutions decreases with decreasing of a_0 and they run into the limit solution in that $t_{f\,\min} = t_{fV}$ and a_0 is the minimum possible value for the landing trajectory. The trajectories with $t_{f\,\min} < t_f \le t_{fV}$ are divided in three phases: initial burn arc, coasting passive arc, and terminal burn arc. These results are in compliance with the Lawden primer vector theory for a uniform gravity field [26]. The spacecraft thrust vector is oriented nearly opposite to the instantaneous velocity vector. For $t_f > t_{fV}$, an optimal trajectory may be designed as a combination of a waiting time $(t_f - t_{fV})$ and trajectory with the minimum required ΔV_x. The results also illustrate the influence of spacecraft thrust-to-weight ratio on lunar landing trajectories. The presented minimum characteristic velocities compare well with required ΔV_x for the Apollo missions [29].

C. Optimal Trajectories with Constraints

Real landing trajectories are often required to satisfy constraints related not only to the terminal conditions (23), but also to constraints

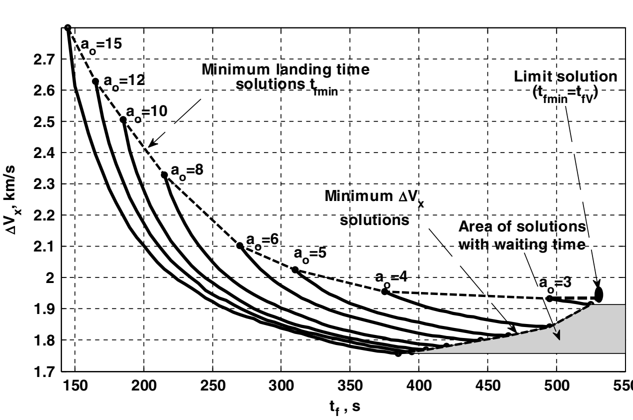

Fig. 5 Required characteristic velocities for optimal unconstrained trajectories.

Table 2 Constraints for landing trajectories

Flight phase	Time interval, s	Constraint: Thrust level	Constraint: Attitude
Terminal	390–400	Constant $f_T = 50\%$	Constant thrust angle $\vartheta = -90$ deg
Transition	360–390	Linearly in time from 100% to 50%	Bound for maximum thrust angle $\vartheta_{\max} = -90\,\mathrm{deg} + (t - 390) \cdot 4\,\mathrm{deg/s}$
Safety profile $h(V_h)$ with free-fall time no less than $t_{\mathrm{AB}} = 40$ s	≤ 360	Functional constraint	Functional constraint

Table 3 Examples of trajectories

Trajectory number	Constraints: Terminal	Constraints: Transition	Constraints: Safety profile	ΔV_x, km/s	Number of burns	Number of nonzero decision variables
1	−	−	−	1.771	2	55
2	+	−	−	1.778	3	54
3	+	+	−	1.824	2	58
4	−	−	+	1.908	3	73
5	+	−	+	1.984	3	81
6	+	+	+	2.079	4	78

on an altitude profile, thrust level, attitude and attitude rate, etc. An example for an inequality interior-point constraint will be given subsequently. Suppose that $t_f = 400$ s, $a_0 = 10$ m/s^2, $\Delta t_i = 2.5$ s, and 360 uniformly distributed pseudoimpulses on the unit circle are used for each segment. Therefore, the number of the decision variables is $(160 \times 360) = 57,600$.

We examine constraints that are given in the Table 2. The first two constraints can be presented in an explicit form through $\Delta V_{i\max}$ and sets of pseudoimpulses for the corresponding segments.

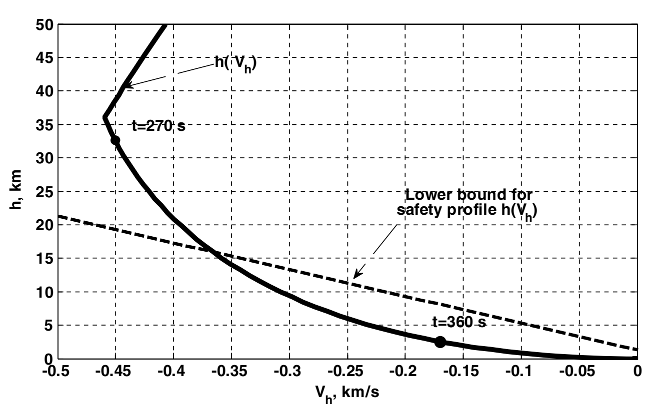

Fig. 6 Profile $h(V_h)$ for an unconstrained trajectory.

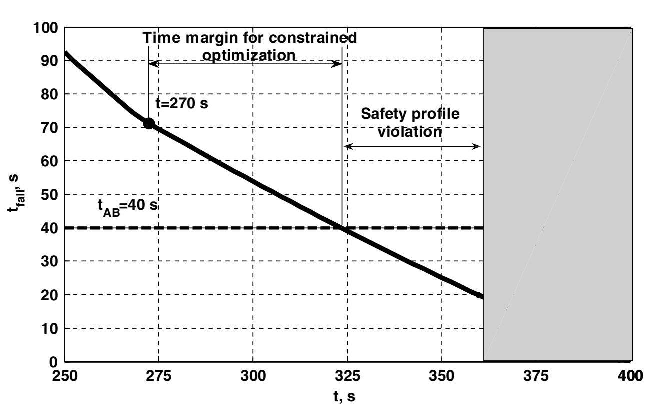

Fig. 7 Free-fall times for an unconstrained trajectory.

The last constraint is related to contingency situations so that the spacecraft should be able to abort the descent process at any time with a free-fall time no less than a safety time t_{AB}. The time t_{AB} is needed for performing operations in a contingency aborting of the descent [30]. We assume that $t_{\mathrm{AB}} = 40$ s (for the Apollo missions, it was $t_{\mathrm{AB}} = 20$ s). For the unconstrained landing trajectory, the safety profile constraint does not hold. The corresponding profile $h(V_h)$ and lower bound of the safety profile are presented in Fig. 6. The free-fall time t_{fall} versus abort time is shown in Fig. 7. Therefore, for a sequence of m adjacent segments (between a segment immediately preceding the first violation of the constraint and up to $t = t_f - t_{\mathrm{AB}} = 360$ s), the following inequalities should be met:

$$Q(h, V_L, V_h, M, t) = -\left(h_l + V_l t_{\mathrm{AB}} - \frac{g_M t_{\mathrm{AB}}^2}{2}\right) \leq 0 \tag{25}$$

where l is a segment number. An additional row of matrix $\mathbf{A}$ (19) and element of vector $\mathbf{b}$ (21) should correspond to each of these inequalities:

$$\mathbf{A}_{n+l,i} = \frac{a_0}{M_i} \Delta t_i \cdot \{(t_l - t_i) + t_{\mathrm{AB}}\}\left[\sin\varphi^{(1)} \quad \sin\varphi^{(2)} \quad \cdots \quad \sin\varphi^{(k)}\right] \tag{26}$$

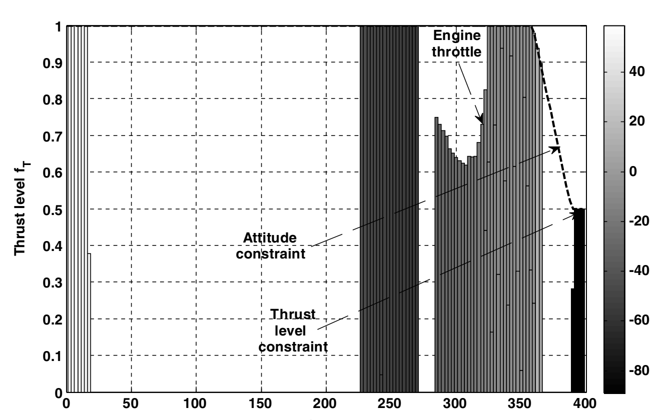

Fig. 8 Thrust profile history for trajectory 6.

$$b_{n+l} = -\left[h_0 - \frac{g_M(t_l + t_{\mathrm{AB}})^2}{2}\right] \tag{27}$$

Suppose that the start time from Eq. (17) is $t_b = 270$ s. It is a time with a margin for the constraint violation time (see Fig. 7). Then $m = 36$ and the matrix $\mathbf{A}$ has a dimension $(160 + 36) \times 57,600$.

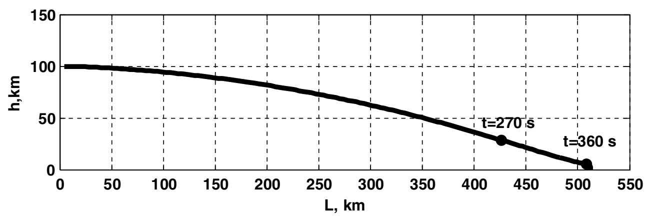

Fig. 9 Landing trajectory in the vertical plane.

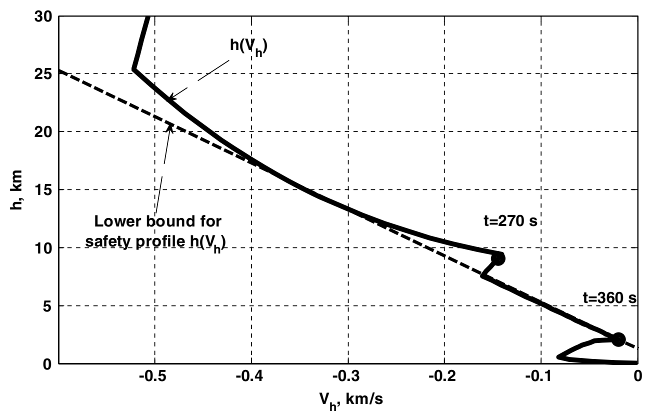

Fig. 10 Safety profile for trajectory 6.

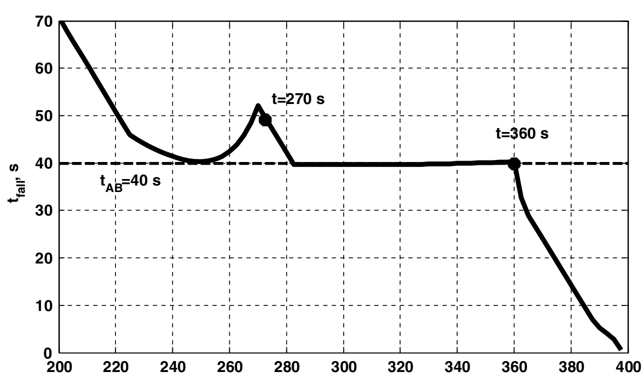

Fig. 11 Free-fall times for trajectory 6.

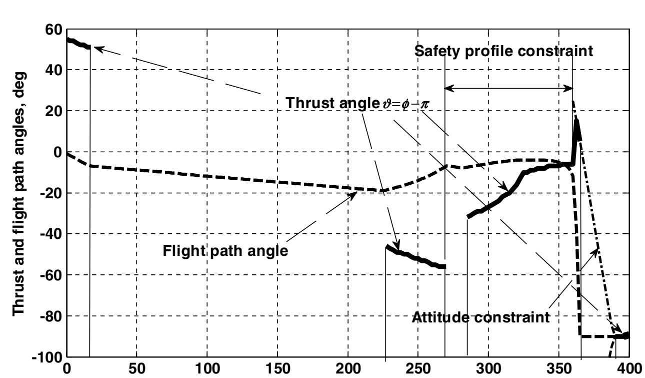

Fig. 12 Thrust angle time history for trajectory 6.

To illustrate trajectory performance effects due to inclusion of each constraint, six trajectories are computed that are given in Table 3. Figures 8–12 present the time histories of several important parameters for trajectory 6. The burn distribution is shown in Fig. 8 as sequences of adjacent segments. Each segment is depicted as a gray-filled rectangle with a height equal to a thrust level. The gray colors of the rectangles correspond to the required thrust angles $\vartheta = \varphi - \pi$ in compliance with the shading scale (the right side in the figure). In fact, it is a four-burn descent. The safety profile is an active constraint. Its effect is easily observed in Figs. 10 and 11: $h(V_h)$ tracks the lower bound of the safety profile. For this phase, the thrust angle ϑ is increased and reaches a local maximum of $\sim$15 deg (see Fig. 12).

V. Conclusions

The purpose of this paper is to present new spacecraft trajectory optimization methods and demonstrate the beneficial features of this approach. The methods are based on a discretization of the trajectory on small segments, and the key idea is to use a discrete approximation for the space of the possible thrust directions by a set of pseudo-impulses for each segment. The methods are attractive for several reasons. First, it is a transformation of the problem to a large-scale linear programming form for which there are effective interior-point algorithms. Second, there is flexible possibility for the trajectory optimization with various operational constraints such as interior-point boundary conditions or inequalities, thrust level, thrust directions, etc. The methods may also be used for determination of a required spacecraft thrust-to-weight ratio in a mission type. Third, the optimal number of burns is automatically determined in the postprocessing of the linear programming solutions. Note that there are also some application possibilities based on iterative techniques for nonlinear problems. In future work, use of the methods for a wider range of nonlinear problems needs to be investigated. We believe that the key idea (i.e., discrete sets for the control space) can be applied to other optimal control problems.

References

[1] Melton, R. G., Lajoie, K. M., and Woodburn, J. W., "Optimum Burn Scheduling for Low-Thrust Orbital Transfers," *Journal of Guidance, Control, and Dynamics*, Vol. 12, No. 1, 1989, pp. 13–18. doi:10.2514/3.20362

[2] Enright, P. J., and Conway, B. A., "Discrete Approximations to Optimal Trajectories Using Direct Transcription and Nonlinear Programming," *Journal of Guidance, Control, and Dynamics*, Vol. 15, No. 4, 1992, pp. 994–1002. doi:10.2514/3.20934

[3] Seywald, H., "Trajectory Optimization Based on Differential Inclusion," *Journal of Guidance, Control, and Dynamics*, Vol. 17, No. 3, 1994, pp. 480–487. doi:10.2514/3.21224

[4] Kluever, C. A., "Low-Thrust Orbit Transfer Guidance Using an Inverse Dynamics Approach," *Journal of Guidance, Control, and Dynamics*, Vol. 18, No. 1, 1995, pp. 187–189. doi:10.2514/3.56676

[5] Coverstone-Carrol, V. L., "Near-Optimal Low-Thrust Trajectories via Micro-Genetic Algorithms," *Journal of Guidance, Control, and Dynamics*, Vol. 20, No. 1, 1997, pp. 196–198. doi:10.2514/2.4020

[6] Kechichian, J. A., "Reformulation of Edelbaum's Low-Thrust Transfer Problem Using Optimal Control Theory," *Journal of Guidance, Control, and Dynamics*, Vol. 20, No. 5, 1997, pp. 988–994. doi:10.2514/2.4145

[7] D'Souza, C. N., "An Optimal Guidance Law for Planetary Landing," *AIAA Guidance, Navigation, and Control Conference*, Pt. 3, AIAA, Reston, VA, Aug. 1997, pp. 1376–1385.

[8] Vasile, M., and Floberghagen, R., "Optimal Trajectories for Lunar Landing Missions," *Advances in the Astronautical Sciences*, Pt. 1, Vol. 100, Univelt, Escondido, CA, 1998, pp. 281–296.

[9] Ulybyshev, Y. P., and Sokolov, A. V., "Many-Revolution, Low-Thrust Maneuvers in Vicinity of Geostationary Orbit," *Journal of Computer and Systems Sciences International*, Vol. 38, No. 2, 1999, pp. 255–261.

[10] Herman, A. L., and Spencer, D. B., "Optimal, Low-Thrust Earth-Orbit Transfers Using Higher-Order Collocation Methods," *Journal of*

Guidance, Control, and Dynamics, Vol. 25, No. 1, 2002, pp. 40–47. doi:10.2514/2.4873

[11] Fahroo, F., and Ross, I. M., "Direct Trajectory Optimization by a Chebyshev Pseudospectral Method," *Journal of Guidance, Control, and Dynamics*, Vol. 25, No. 1, 2002, pp. 160–167. doi:10.2514/2.4862

[12] Petropoulos, A., "Low-Thrust Orbit Transfers Using Candidate Lyapunov Functions with a Mechanism for Coasting," AIAA/AAS Astrodynamics Specialist Conference and Exhibit, Providence, RI, AIAA Paper 2004-5089, Aug. 2004.

[13] Haberkorn, T., Martinon, P., and Gergaud, J., "Low Thrust Minimum-Fuel Orbital Transfer: A Homotopic Approach," *Journal of Guidance, Control, and Dynamics*, Vol. 27, No. 6, 2004, pp. 1046–1060. doi:10.2514/1.4022

[14] Ranieri, C. L., and Ocampo, C. A., "Optimization of Roundtrip, Time-Constrained, Finite Burn Trajectories via an Indirect Method," *Journal of Guidance, Control, and Dynamics*, Vol. 28, No. 2, 2005, pp. 306–314. doi:10.2514/1.5540

[15] Ross, I. M., Gong, Q., and Sekhavat, P., "Low-Thrust, High-Accuracy Trajectory Optimization," *Journal of Guidance, Control, and Dynamics*, Vol. 30, No. 4, 2007, pp. 921–933. doi:10.2514/1.23181

[16] Ulybyshev, Y., "Continuous Thrust Orbit Transfer Optimization Using Large-Scale Linear Programming," *Journal of Guidance, Control, and Dynamics*, Vol. 30, No. 2, 2007, pp. 427–436. doi:10.2514/1.22642

[17] Ulybyshev, Y., "Optimization of Multi-Mode Rendezvous Trajectories with Constraints," *Cosmic Research (Translation of Kosmicheskie Issledovaniya)*, Vol. 46, No. 2, 2008, pp. 133–147. doi:10.1134/S0010952508020056

[18] Ulybyshev, Y., "Concept of Pseudoimpulses for Spacecraft Trajectory Optimization," *Polyot (Flight)*, No. 2, 2008, pp. 52–60 (in Russian).

[19] Pontryagin, L. S., Boltyanskii, V. G., Gamkrelize, R. V., and Mishchenko, E. F., *The Mathematical Theory of Optimal Processes*, Wiley, New York, 1962, Chap. 2.

[20] Betts, J., "Survey of Numerical Methods for Trajectory Optimization," *Journal of Guidance, Control, and Dynamics*, Vol. 21, No. 2, 1998, pp. 193–207. doi:10.2514/2.4231

[21] Wright, S., *Primal-Dual Interior Point Methods*, Society for Industrial and Applied Mathematics, Philadelphia, 1997, Chap. 2.

[22] Rao, S. S., and Mulkay, E. L., "Engineering Design Optimization Using Interior-Point Algorithms," *AIAA Journal*, Vol. 38, No. 11, 2000, pp. 2127–2132. doi:10.2514/2.875

[23] Wright, M. H., "The Interior-Point Revolution in Optimization: History, Recent Developments, and Lasting Consequences," *Bulletin of the American Mathematical Society*, Vol. 42, No. 1, 2004, pp. 39–56. doi:10.1090/S0273-0979-04-01040-7

[24] Battin, R. H., *An Introduction to the Mathematics and Methods of Astrodynamics*, AIAA, New York, 1999, Chaps. 9.4, 10.3.

[25] *MATLAB® Users Guide*, The Math Works, Inc., Natick, MA, 2003, Chap. 16.

[26] Lawden, D. F., *Optimal Trajectories for Space Navigation*, Butterworths, London, 1963, Chap. 5.

[27] Bryson, A. E., Jr., and Ho, Y.-C., *Applied Optimal Control*, Hemisphere, New York, 1975, Chap. 7.3.

[28] Marchand, B. G., Howell, K. C., and Wilson, R. S., "Improved Corrections Process for Constrained Trajectory Design in the *n*-Body Problem," *Journal of Spacecraft and Rockets*, Vol. 44, No. 4, 2007, pp. 884–897. doi:10.2514/1.27205

[29] Wilhite, A. W., Wagner, J., Tolson, R., and Mazur, M. M., "Lunar Module Descent Mission Design," AIAA/AAS Astrodynamics Specialist Conference and Exhibit, Honolulu, HI, AIAA Paper 2008-6939, Aug. 2008, p. 14.

[30] Bennett, F. V., "Apollo Experience Report—Mission Planning for Lunar Module Descent and Ascent," NASA TN D–6846, 1972, http://ntrs.nasa.gov/archive/nasa/casi.ntrs.nasa.gov/19720018205_1972018205.pdf [retrieved 24 Mar. 2009].